Structural and Multidisciplinary Optimization (2022) 65:38
https://doi.org/10.1007/s00158-021-03124-6

RESEARCH PAPER

Topological control for 2D minimum compliance topology optimization using SIMP method

Qianglong Wang[1,2] · Haitao Han[1,2] · Chong Wang[1] · Zhenyu Liu[1,2]

Received: 9 August 2021 / Revised: 12 November 2021 / Accepted: 26 November 2021 / Published online: 10 January 2022

Abstract

Topological constraints have recently been introduced to structural topology optimization by the BESO method. However, for the classical and widely used SIMP-type optimization method, an implicit and continuously changing variable cannot express the topological characteristics directly during the optimization process. This is partly caused by missing well-defined boundaries to compute topological characteristics. To introduce topological constraints into the SIMP-type method, an auxiliary discrete expression of structural boundaries through the volume preservation projection method is used to compute topological characteristics, that is, the genus or number of holes. A topological control methodology based on persistence homology, a numerical calculation idea derived from topological data analysis, is introduced in this paper to implement topological constraints. With the help of the design space progressive restriction method, the proposed methodology shows that for the 2D static minimum compliance optimization problem, the inequality constraints on the number of holes can be satisfied. The effectiveness of the proposed topological control method for the SIMP-type framework is illustrated by several numerical examples.

Keywords Topological control · Genus · Persistence homology · Projection · Filtering

1 Introduction

The basic and most important idea for structural design is where to put the right holes, and the art of hole- design determines the pros and cons of the structure (Bendsøe and Sigmund, 2003). For a given design space and specified design constraint, the topology optimization method (Bendsøe and Kikuchi, 1988) has been proved to be a powerful inverse design methodology for conceptual design and has been extended in many physical inverse design problems (Lin et al., 2019; Sigmund, 2004; Andkjær and Sigmund, 2011; Deng et al., 2013), being especially mature for static structural minimum compliance optimization, which has been integrated into in many commercial FEM software programs in recent years.

Literally, topology optimization means that the method can optimize the structural topology. The genus is a parameter used to express the characteristics of a structure. For the 2D case, the genus is simplified as the number of holes or cavities. Controlling the topology for the 2D case is equivalent to controlling the number of holes in structure. There are two ways to control the number of holes for topology optimization: the direct method and the indirect method. For the direct method, a typical strategy is to add topological constraints explicitly to the optimization model (i.e., limit the maximum number of holes). Correspondingly, the indirect method controls the topology through adjustment of the optimization parameters.

Topological control, also called structural complexity control (SCC), has been considered as a constraint for ESO (evolutionary structural optimization)- type topology optimization methods (Kim et al., 2000). The inequality constraint on the number of *cavities,* defined as enclosed voids surrounded by elements, was integrated into the optimization model. A novel but indirect topological constraint for enclosed voids restriction for additive manufacturing was

Responsible Editor: Emilio Carlos Nelli Silva

✉ Zhenyu Liu
liuzy@ciomp.ac.cn

[1] Fine Mechanics and Physics (CIOMP), Changchun Institute of Optics, Chinese Academy of Science, Changchun 130033, China

[2] School of Optoelectronics, University of Chinese Academy of Sciences, Beijing 100049, China

introduced though the virtual temperature method (Liu et al., 2015). The structural connectivity was controlled by introducing a new auxiliary temperature field. With the foundation of graph theory and set theory (Zhao et al., 2020), the number and size of interior holes can be controlled by updated BESO (soft-kill bi-directional evolutionary structural optimization) method, and the conception of structural complexity control was proposed. Genus, the concept that describes topological invariant was used to directly control the maximum number of holes for the design domain. The basement optimization framework was also the BESO method and the hole calculation method was the Gauss-Bonnet method (Han et al., 2021).

One of the most widely used indirect topological control concepts is length scale control (Lazarov et al., 2016; Zhou et al., 2015; Guest, 2008; Guest and Prevost, 2006; Guest et al., 2004). Based on the classical SIMP method, several works have proved beneficial for controlling the relative material distribution, such as adding slope constraints (Joakim et al., 1998), imposing extra cost functions on the length scale (Poulsen, 2003) and applying circular test regions with radii equal to the maximum design length scale constraints (Guest, 2008). Combining extra design fields and Heaviside projection methods, one can choose suitable parameters to create a more variable topology for manufacturing constraints and design purposes (Lazarov and Sigmund, 2011; Wang et al., 2010; Lazarov and Wang, 2017).

To implement the topological constraint directly for the SIMP method, the first step should be to define the hole by an explicit boundary via a well-defined 0–1 auxiliary discrete design variable; the second step would then be to find the algorithm for calculating the number of holes; and the third step would be to carry out the methodology for controlling the number of holes or genus.

A direct method for obtaining a boundary well-defined discrete auxiliary 0–1 variable could be to calculate a threshold value, for design variables that are larger than the threshold value is projected as 1 and smaller as 0. The threshold value would be unique if the volume constraint is introduced in this step. First, the value can be calculated in the same way using the bisection method of the classical OC update strategy. Second, after the first projection step and obtaining discrete variables, either the Gauss-Bonnet method or Fire-Burning method can be used to count the number of holes. Third, the filtering design variable method is proposed by tuning the size of the filter radius. The concept came from persistence homology, and a continuous parameter acting on the target geometry would gradually smooth the holes and cavities of its geometric structure. Thus, this continuous parameter is chosen as the filter radius in this paper.

In this paper, a topological control methodology is proposed in 2D structural minimum compliance optimization problems based on the classical SIMP optimization model. The paper is composed as follows. In Sect. Methodology, we define the basic optimization framework and list a detailed description of the proposed method. In Sect. Numerical Examples, we show some numerical examples of this method. Section Discussion and Sect. Conclusion offer a discussion and the conclusions of the methodology.

2 Methodology

The computational optimization model in this paper is as follows:

$$\begin{aligned} \min_{\rho_e} \quad & c(\rho) = U^T K U = \sum_{e=1}^{N} (\rho_e)^p u_e^T k_0 u_e \\ \textit{subject to} \quad & KU = F \qquad \textit{in} \quad \Omega \\ & \sum_{e=1}^{N} \rho_e V_e - V^* \le 0 \quad V^* = \alpha V_0 \\ & 0 < \rho_{\min} \le \rho_e \le 1 \\ & g \le g_c \end{aligned} \tag{1}$$

where c is the compliance, and U and F are the global displacement and force vectors, respectively. K is the global stiffness matrix. u_e is the element displacement vector, k_0 is the element stiffness matrix for an element with unit Young's modulus, and ρ is the vector for design variables (i.e., the element densities). N is the number of elements used for discretizing the design domain, V_e is the unit element volume, V_0 is the total volume for the design domain Ω, and α is the volume fraction. For a more numerically stable iteration, we choose $\rho_{\min} = 0.001$. The genus g of a structure equals the number of holes the during iterative computation process, and g_c is the target maximum constraint number of holes. The calculation method for the number of holes g is discussed in the next sections. We consider the genus in the 2D case to be holes enclosed by solids. Thus, the number of holes is calculated and controlled.

Two standard structural optimization problems are used to illustrate the effect of the proposed optimization method,

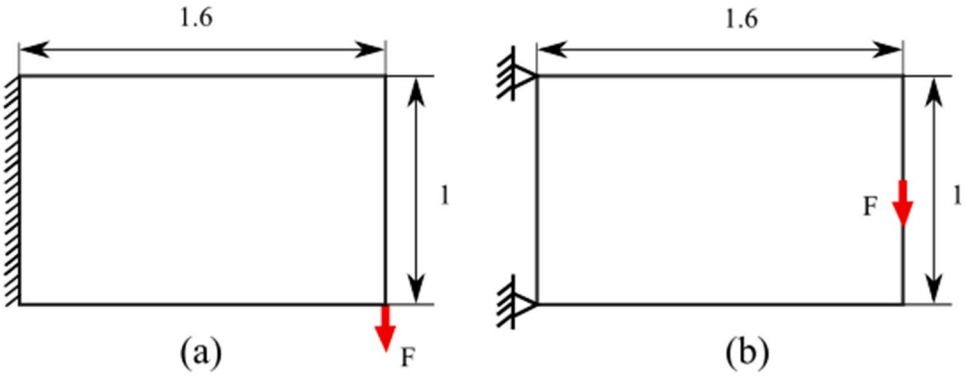

Fig. 1 Sketch of short cantilever beam, fixed displacement constraints and load conditions; **a** Left boundary is fixed, and a unit load is applied for the bottom right; **b** The left two points are fixed and an unit load is applied for the middle right

where the design domain, the boundary conditions, and the external load for the cantilever beam are illustrated in Fig. 1. The target of the optimization problem is to find the optimal material distribution under the inequality constraint on the number of holes.

2.1 Holes and counting the number of holes in the SIMP method

A hole can be intuitively interpreted as a region enclosed by a solid for a two-dimensional design region (Edelsbrunner, 2014). Therefore, the definition of holes requires clearly distinguishing between the solid domains (shown as black areas in this paper) and void domains (shown as white areas).

However, the classical SIMP-type method (Sigmund, 2001) adopts the relaxation method for topological evolution to avoid large-scale 0–1 discrete optimization problem. The optimized intermediate solution and final convergent solution are based on the implicit description of the structural topology which is not a fully 0–1 discretized computational result. Thus, no direct and explicit expression of holes exists for the classical topology optimization method.

Two problems need to be solved to define and constrain the number of holes during the optimization process. First, a method should be defined to project the continuous design variable to 0 and 1, to express the boundary explicitly. Second, a numerical algorithm is needed to calculate the number of holes corresponding to the hole expression.

2.2 Volume preservation discrete projection

To count the number of holes for a given distribution of a reasonable combination of design variables, a straightforward way is to project the continuous value of the design variable $\rho \in [\rho_{\min}, 1]$ to the auxiliary discrete 0–1 expression. Clearly there are many possible ways to implement projection operation (Li and Khandelwal, 2015; Guest, 2015; Zhou et al., 2014; Guest et al., 2011; Wang et al., 2010; Kawamoto et al., 2010; Guest et al., 2004; Ferrari and Sigmund, 2020; Xu et al., 2009), but the counting procedure needs a fully 0–1 discrete expression of design field. Consider the equality constraint on the material volume, we chose to simplify this step. Using bisected method to find the threshold value to get a volume preservation discrete projection (VPDP) of design variables ρ_V. The design variables exceeding the projection threshold ρ_{th} are projected as solid (1), and those smaller than or equal to the projection threshold are projected as void (0). The sum of the discrete auxiliary variable ρ_V and design variable ρ is kept as constant before and after the discrete projection procedure. Equation 2 illustrates the formula of VPDP.

$$\begin{aligned} \rho_V &= \begin{cases} 1 & \rho > \rho_{th} \\ 0 & \rho \le \rho_{th} \end{cases} \\ \sum \rho_V &= \sum \rho \end{aligned} \tag{2}$$

Figure 2 shows the results of the VPDP for a given optimization variable of the iteration step, where the left column shows the figure of the design variable ρ before discrete projection and the right column shows the projected discrete auxiliary variable ρ_V.

2.3 Hole expression in the 2D case

There are three parts of the auxiliary discrete design domain for the 2D case after discrete projection: Ω_S (i.e., the solid domain), Ω_H (i.e., the hole domain) and Ω_B (i.e., the void domain, which intersects with the design boundary). The number of Ω_H indicates the structure of the genus (i.e., the number of holes in this paper).

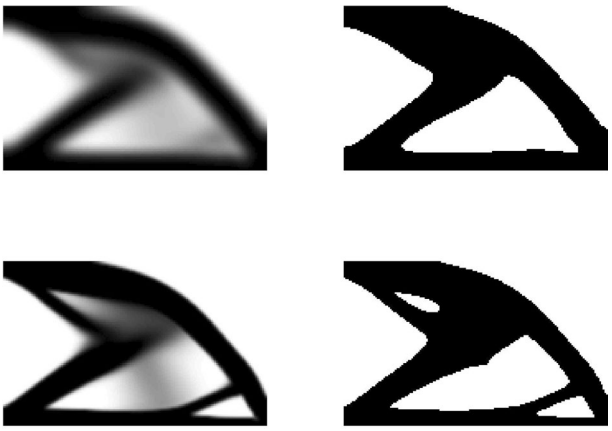

Fig. 2 Examples of the VPDP, where the target volume fraction is 0.5; *Left*: Original design variable ρ, *Right*: Projected discrete auxiliary variable ρ_{V}

Two examples of one hole and three holes are given in Fig. 3. The value of domain Ω_{H}(value of Ω_{H} is defined as g in this paper) affects the topology. But the existence of void domains intersecting with boundaries does not affect the topology. Thus, the value of domain Ω_{B} (the value of Ω_{B} is defined as c in this paper) would not be counted and the constraint for the number of holes can be introduced to the optimization model as an inequality constraint.

2.4 Counting the number of holes: the Fire-Burning method

Information on the number of holes can be obtained using either the Gauss-Bonnet method (GBM) or the Fire-Burning method (FBM) (Han et al., 2021). The computational cost of the GBM is lower than that of the FBM. To illustrate the subdomain information of holes, the FBM is used in this paper because the GBM cannot provide the subdomain information.

The algorithm for the FBM is mainly based on the connection matrix. The definition of the connection matrix and strategy algorithm for the FBM is illustrated in Fig. 4 and Fig. 5. For element a_{ij} in connection matrix A, if a_{ij}= 1,then we consider that element i and element j are connected to each other; if a_{ij}= 0,then element i and element j would be considered as disconnected state. The concepts of two kinds of connective relationships and the corresponding connection matrix are shown in Fig. 4. For the structured square mesh, the connective relation in Fig. 4a is adopted in this paper and its connection matrix is shown in Fig. 4b.

After the connection matrix is defined, we show an example about how FBM works for a design domain with 9 squared mesh elements in Fig. 5. Figure 5a is the connection matrix for discrete domain in Fig. 5b. The key strategy is to traverse the connection matrix with an arbitrary starting point until all the void subdomains are identified. We consider that the void domain conclude element $Void$=$\{$ e2 e3 e7 e8 e9 $\}$; and after the FBM procedure, the two voids group $Subvoid\_1 = \{e2, e3\}$ $Subvoid\_2 = \{e7, e8, e9\}$ can be obtained. Figure 5c show the detail flow for this algorithm.

2.5 Implementing the genus constraint using the persistence homology

The concept underlying topological constraint in this paper is derived from persistent homology in computational topology. Persistent Homology (PH) is a method used in

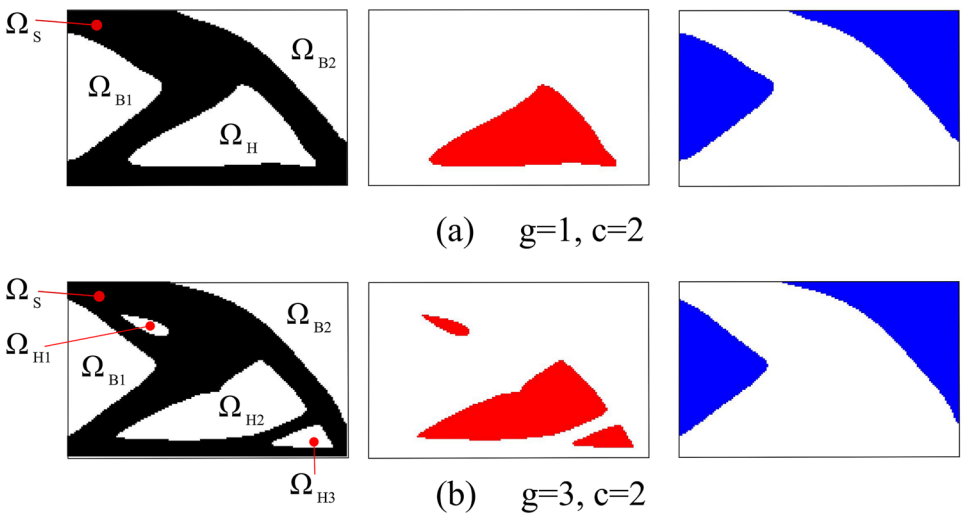

Fig. 3 The definition of Ω_S, Ω_{H} and Ω_{B}. The red areas in the middle column show Ω_{H}, and the blue areas in the right column show Ω_{B}. g is the number of holes

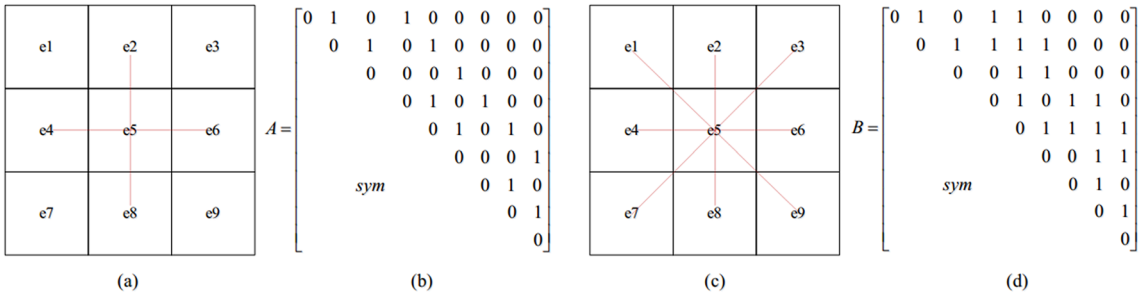

Fig. 4 Adjacency relations for the structural square mesh. **a** Diagonal elements are not considered connectivity elements; **b** Connection matrix for Fig. 4a; **c** Diagonal elements are considered connectivity elements; **d** Connection matrix for Fig. 4c

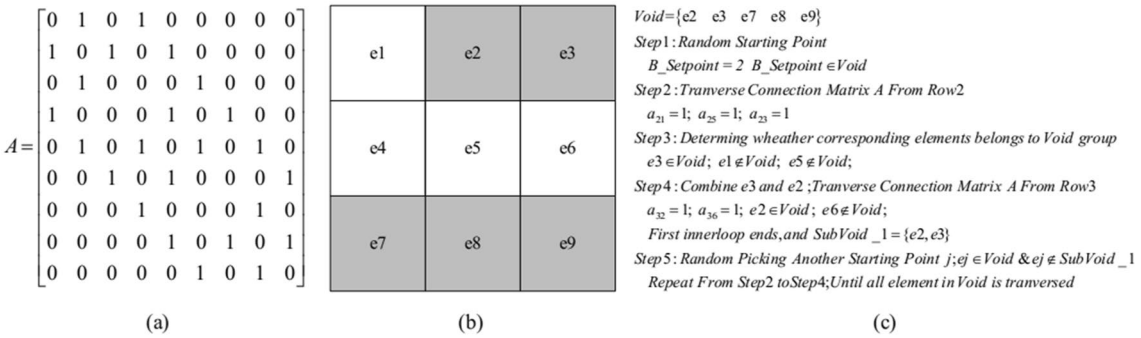

Fig. 5 Schematic of the Fire-Burning method

topological data analysis to study the qualitative features of data that persist across multiple scales (Otter et al., 2017; Fugacci et al., 2016; Carlsson, 2009, 2020; H. Edelsbrunner and Harer, 2008). The core idea is to detect more persistent features over a wide range of spatial scales using filter functions with different spatial scales.

The filter function in the PH calculation corresponds to the density filter function in the SIMP method. In essence, one can modify a structural topology by adjusting the parameters of the filter radius. For the structural topology optimization method, the number of holes in the optimized results decreases monotonically with increasing the radius by filtering the design variables.

The results of the design variables and the binarized hole calculations for different constant filter radii (*rmin*) of the density filter are given in Fig. 6. The boundary and load condition are defined in Fig. 1a. The first column presents the original design variables after optimization, the second column presents the projected discrete auxiliary variable via VPDP, and the third column presents the hole conditions calculated through the FBM.

Figure 6 shows how the filter function, the idea derived from the PH, affects the structural topology gradually with varying filter radius (adjustable parameters in topology optimization). This is the core of the computational strategy for the proposed topological control methodology.

2.6 Design space progressive restriction method (DSPRM)-a strategy for obtaining binary design solutions under large density filter radius

The design strategy of simply increasing the filter radius for the original design variable leads to the existence of more intermediate variables between 0 and 1 in the iterative process and optimized result. The existence of intermediate variables lacks manufacturability in engineering design, especially in structural optimization design. Note that in Fig. 6f, due to the smoothing effect of the larger filter radius function, the design variable close to 1 could be redistributed to the neighborhoods element, and the full design thus cannot converge to the nearly 0–1 result. One way to solve this problem is to progressive restrict the design space in the iterative update strategy based on the classical OC optimization algorithm (Sigmund, 2001) so that the

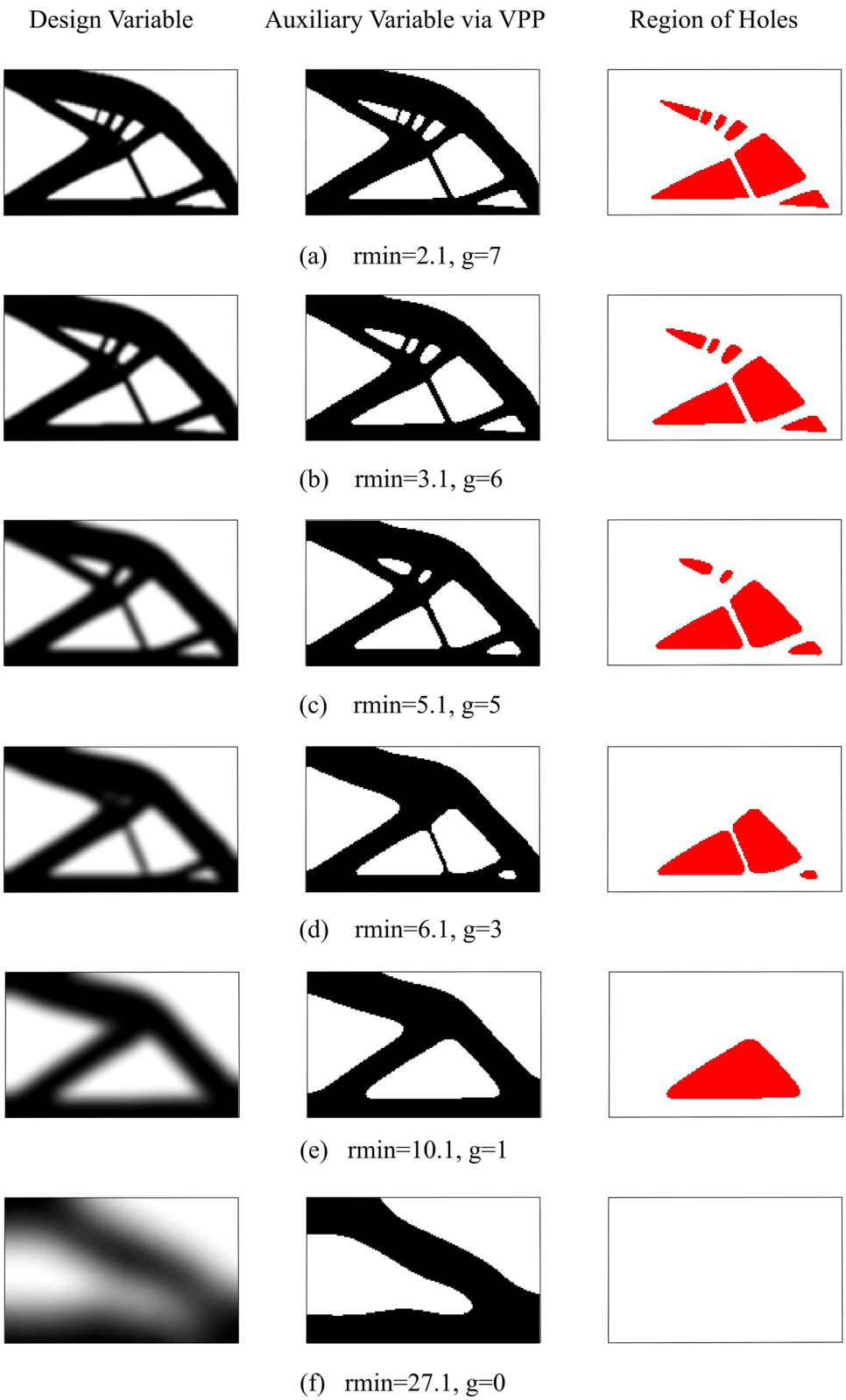

Fig. 6 Effect of the density filter radius on the final optimized topology. mesh: *160*100*, volume fraction equals *0.5*, penalty factor $p = 3$, and maxiter $iter_{\max} = 100$

design variables that are larger than 0.5 can only vary in the interval close to 1.

The design space of the design variable ρ located in an n-dimensional super-cubic domain R^n, where n is the number of design variables, $R \in [\rho_{\min}, 1]$. Taking the two design variables as an example, the key strategy is illustrated in Fig. 7. The lower limit for variables that tend to 1 is gradually rises. By gradually increasing the allowable lower limit through the above method, the intermediate optimized solution converges to 1 and stabilizes near solid 1, thus achieving the constraint goal of stable control of extreme hole constraints. Specifically, the following algorithm in Eq. 3 is used to implement the update strategy during the OC update procedure.

$$\rho^n(\rho^n > 0.5) = \begin{cases} 0.5 + \min(0.499, ratio * n); & if\ (0.5 + \min(0.499, ratio * n)) > \rho^n(\rho^n > 0.5) \\ \rho^n(\rho^n > 0.5); & if\ (0.5 + \min(0.499, ratio * n)) \le \rho^n(\rho^n > 0.5) \\ 1; & if\ \max\left((0.5 + \min(0.499, ratio * n)), \rho^n(\rho^n > 0.5)\right) > 1 \end{cases} \tag{3}$$

where $\rho^n(\rho^n > 0.5)$ is part of the design variables that are larger than 0.5 for iteration step n. The selection of the proportional parameter *ratio* depends on how fast one would like to push the lowest bound of design space to the upper limit.

2.7 Optimization framework

In summary, the algorithm in this paper explicitly calculates the number of holes through the VPDP and the FBM during optimization process. To accelerate the computation time, a series of matrices is calculated using different filter radius before optimization. When the number of calculated holes exceeds the current number of holes constrained by the design, according to the previous analysis, gradually increasing the filter radius and redistributing the design variables suppresses the generation of new holes to a certain extent. With the help of the DSPRM, the binary design solution requirement under a large filter radius can also be satisfied by limiting the lower limit of the design variables in the OC iteration upgrade procedure. We choose the maximum iteration number as the convergence criterial, if the iteration number exceeds the pre-defined maximum iteration number, the loops end.

The main algorithm computational step of the proposed topological control method is given in Fig. 8 and the optimization procedure can be described as follows:

- Initialize the design variables and generate the global filter matrix with different filter radii H^{r_n}, $r_n = 1.1 + (n-1)^{1.3}; n = 1:20$. That is, the radius to generate the filter matrix grows sequentially as follows: filter matrix $H^{r_1=1.1}$ for radius $r = 1.1$ when $n = 1$; filter matrix $H^{r_2=2.1}$ for radius $r = 2.1$ when $n = 2$; filter matrix $H^{r_3=3.56}$ for radius $r = 3.56$ when $n = 3$. etc.
- Calculate the sensitivity of objection, taking the sensitivity filter the using fixed filter radius $r = 1.1$ to smooth the sensitivity. Update the design variables using the filtered sensitivity and obtain new design variables ρ_{new}.Then, the DSPRM strategy would be integrated into the OC procedure;

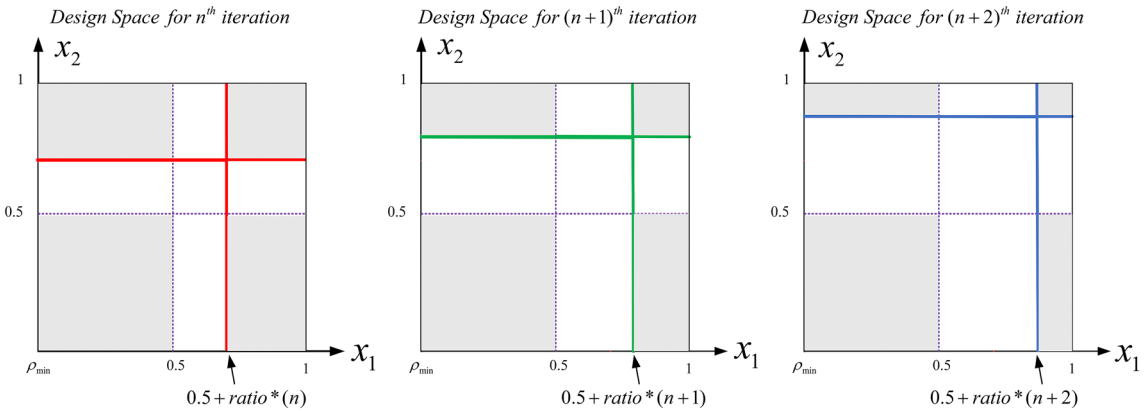

Fig. 7 Schematic of the DSPRM for two design variables; the shadow line area is the allowable design space

- Based on new design variables ρ_{new}, obtain the projected auxiliary discrete 0–1 variables ρ_V; With the help of the FBM, analyses whether ρ_V satisfies the hole constraint.
- If the hole constraints are satisfied, take ρ_{new} as a new value for the next iteration.
- If ρ_V cannot satisfy the hole constraints, then the design variables ρ_{new} are redistributed using the filter matrix. Calculate ρ_{new}^j and its projected auxiliary discrete variables ρ_V^j step by step. Calculate the number of holes of ρ_V^j through the FBM; until the projected auxiliary discrete variables ρ_V^j, $1 \le j \le n$, satisfy the hole constraints for the *j-th* step.
- Take ρ_{new}^j as the new value for the next iteration

3 Numerical examples

In this section, the effectiveness of the proposed algorithm is illustrated with the calculation example of a cantilever beam as defined in Sect. Methodology. The discretized computational region is calculated with a square mesh, and the analysis is calculated by interpolation of the element design variables with a cell load size of 1.

3.1 Results of the bottom-load condition

This section presents the example calculation of the discussed algorithm for Fig. 1a with a computational mesh of 160*100 and a volume fraction of 0.5. Figure 9 shows the optimized design variable (*left column*), the auxiliary discrete variable via VPDP (*middle column*) and the region of calculated holes (*right column*) using only sensitivity filter with the radius $r = 1.1$. And the topological constraint algorithm is not implemented into this numerical example. For the load condition in Fig. 1a, the total calculated number of holes is 44, and for the load condition in Fig. 1b the calculated number of holes is 72.

Figure 10 shows the optimized results ρ with the number of holes inequality constraint well-satisfied. The hole maximum constraint number g_c change from 0 to 11. The chosen value of the factor *ratio* for the restricted design space is 0.002. Obviously, the design variable ρ and projected discrete variable ρ_V are to be identical to each other after 250 steps. The maximum iteration number is 320 in this paper. And that number aim to show that the design variable remains unchanged and the objection value are constant after 250 steps.

Figure 11 shows the objective value and hole growth properties for the SIMP-type method under the 5-hole constraint. As the iteration began, there were no hole areas. Figure 12 shows the inner step number of iterations for redistributed design variable under the same hole constraint as in Fig. 11. And Fig. 13 gives the details of the topological constraint condition at the outer iteration of step 31. At the first beginning of step31, the number of holes calculated from auxiliary discrete(middle column) variable for initial design variable ρ_A (left column) equals to 7 and exceeds the target 5-hole constraint. So, the radius increases gradually and until the hole constraint is satisfied. And ρ_E is taken in the iteration process as the initial value for the next upgrade procedure.

Table. 1 and Fig. 14 list the objective strain energy for the constraint on different number of holes. When the hole constraint cannot be satisfied, a larger filter radius is required to redistribute the material, which is the reason why in Fig. 12, the number of intermediate iterations oscillates several times. The oscillation can be clearly seen from the history of iterations in Fig. 14.

3.2 Results of the middle-load condition

This section shows the example calculation of the discussed algorithm for Fig. 1b with a computational mesh of 160*100 and a volume fraction of 0.5. Figure 15 shows the maximum hole constraint number g_c from 0 to 11 and its optimized result ρ. The chosen scale factor *ratio* for the progressive restriction strategy is 0.002.

It can be seen from Fig. 15 that asymmetric computational solutions do not exist in the design space in the case of symmetric boundary conditions and symmetric loads. In addition, some of the solutions with larger hole constraints are subject to the hole generation performance, and they eventually converge to solutions with less than the target hole constraint. That is, the final number of generated holes is less than or equal to the target hole constraint.

Table. 2 and Fig. 16 show the objective strain energy for the constraint on various number of holes.

4 Discussion

A fixed mesh and constant volume fraction are used in Sect. Numerical Examples to illustrate how the proposed method works for constrained number of holes. The discussion

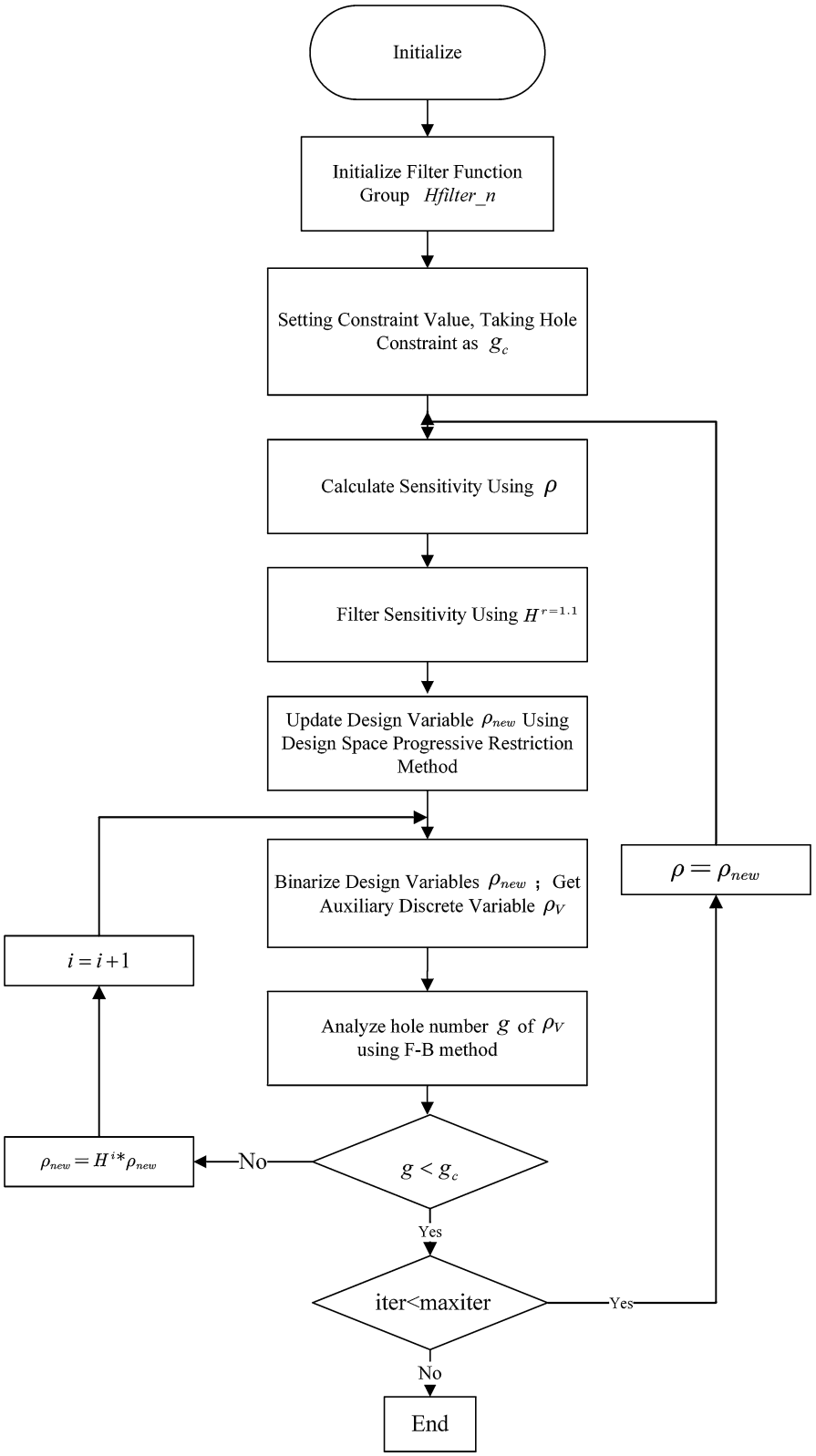

Fig. 8 Algorithm computational iteration flow chart

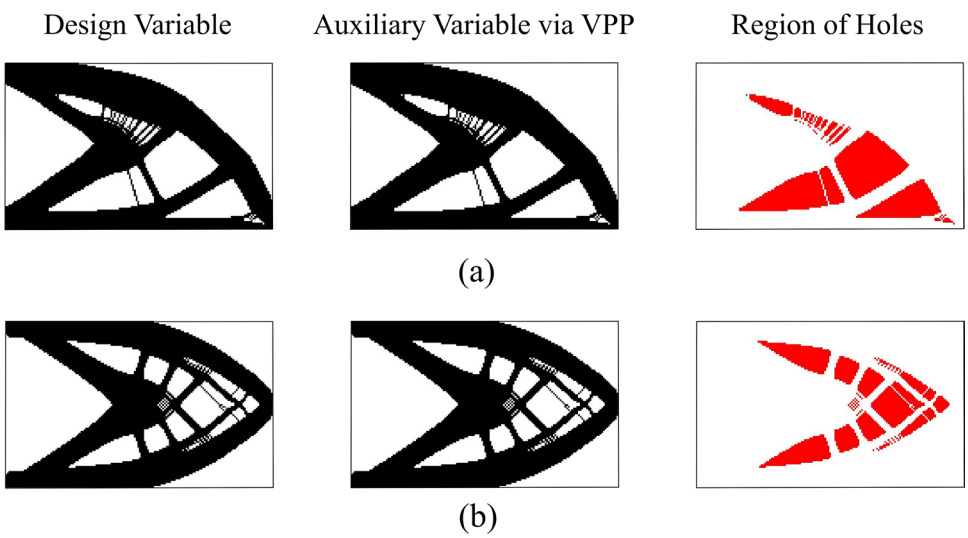

Fig. 9 Results without topological constraint by a constant sensitivity filter radius r = 1.1. Optimized design variable (left column); Auxiliary discrete variable via VPDP (middle column); Hole areas (right column)

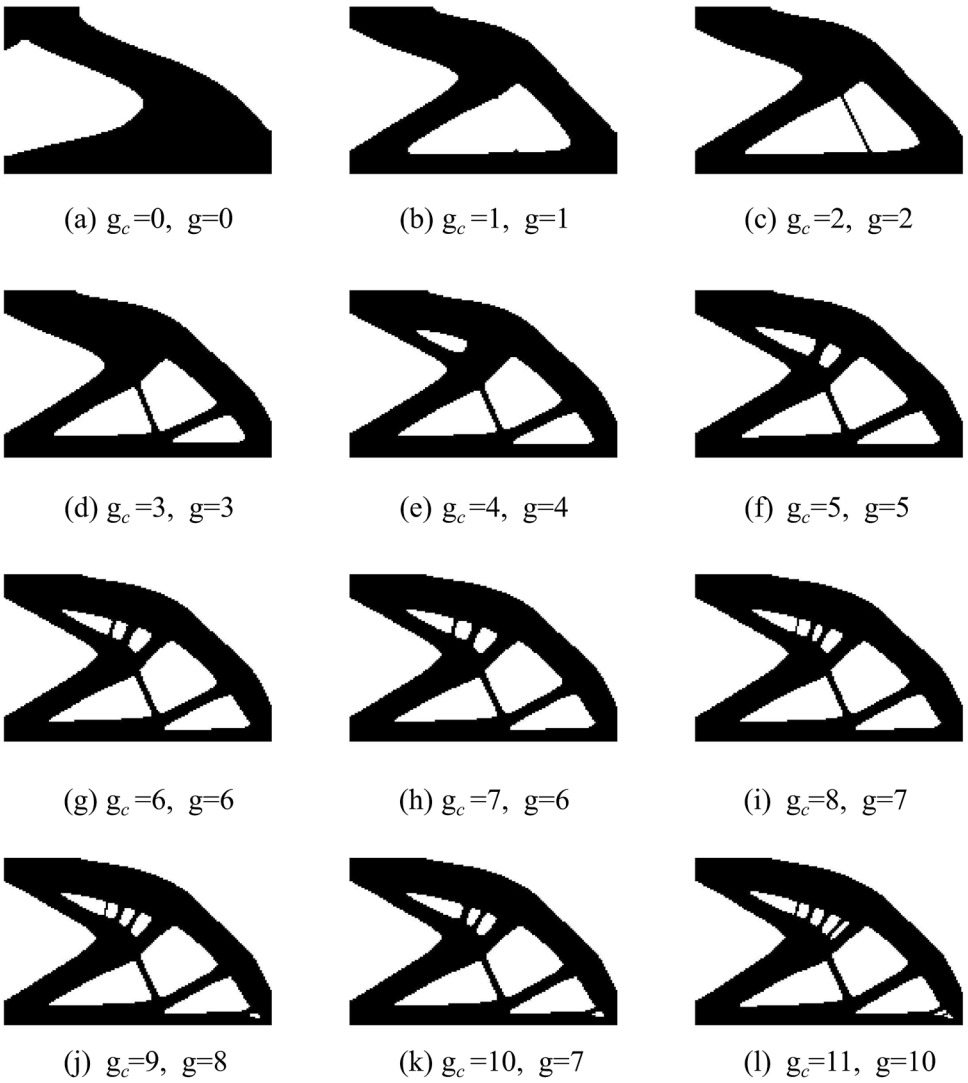

Fig. 10 Hole-constrained results after optimization. The load condition is defined in Fig. 1a. g_c is the maximum hole constraint number, and g is the number of the holes of calculated result

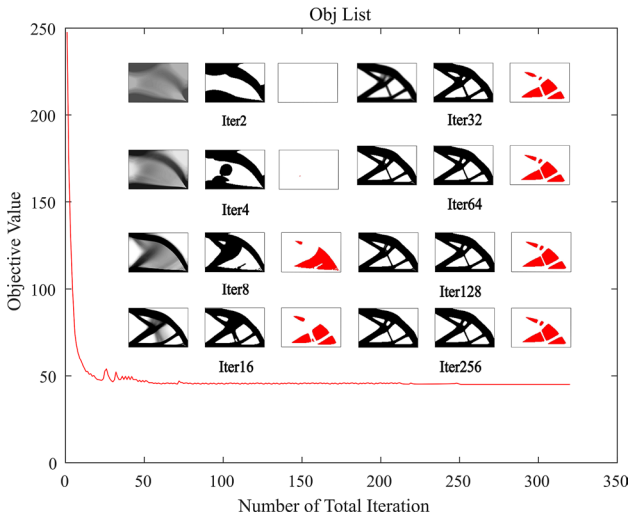

Fig. 11 Iterative history curves under the 5-hole constraints; The original design variables, volume preserving discrete projection design variables and corresponding hole analysis results are given for each iteration step

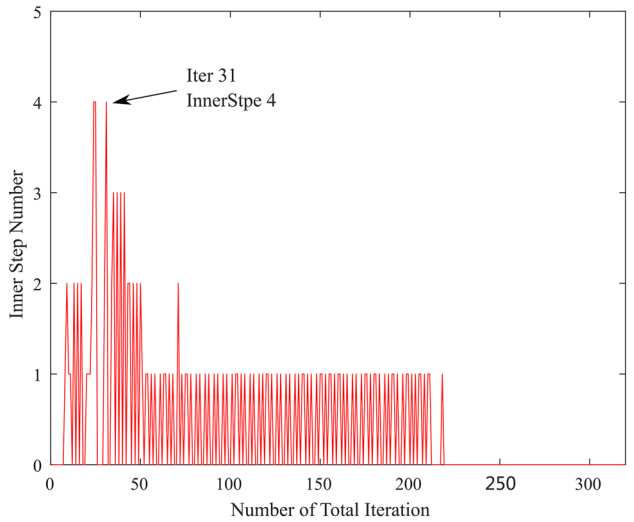

Fig. 12 Intermediate iteration step history iteration curve. For iteration 31, the algorithm redistributes the design variable 4 times to satisfy the hole constraint

below shows the topological control effect when these two factors are varied.

4.1 Mesh dependence

A suitable inverse design algorithm should be mesh-independent, and it is reliable if the optimized design solution can converge on either a large-scale or a small-scale mesh. For a mesh that can generate holes for target number, the hole control algorithm should also be controlled at that level. Figure 17 and Fig. 18 illustrate the optimized result under the 5-hole constraint with the same volume fraction 0.5 for 80*50 mesh density, 160*100 mesh density and 320*200 mesh density, respectively. Obviously, the hole control algorithm generates a convergent result for a finer mesh.

4.2 Discussion of the calculation results at different volume fraction

Similarly, the material distribution at different volume fractions also affects the generation and distribution of the final topology. Figure 19 gives the optimized result of material fractions from 0.2 to 0.6 for the load conditions of Fig. 1a with the 5-hole constraints applied. When the volume fraction is 0.2, a rod connected to the fixed edge of the constraint as shown in Fig. 19a is generated, because the intersection of the class of rods with the boundary is not considered as a hole; therefore, the computational results in this example also satisfy the constraint condition of the 5-hole constraint.

Figure 20 shows the result for the load conditions of Fig. 1b under different volume fraction. For load condition Fig. 1b, the optimized result with the variable volume fraction is much more similar than that for Fig. 1a.

4.3 Further Discussion

The basic premise of this paper is that the volume constant constraints are tightly supported, so that the design variables always wander in the boundary of the volume constraints during the optimization process. Thus, the suitability of the

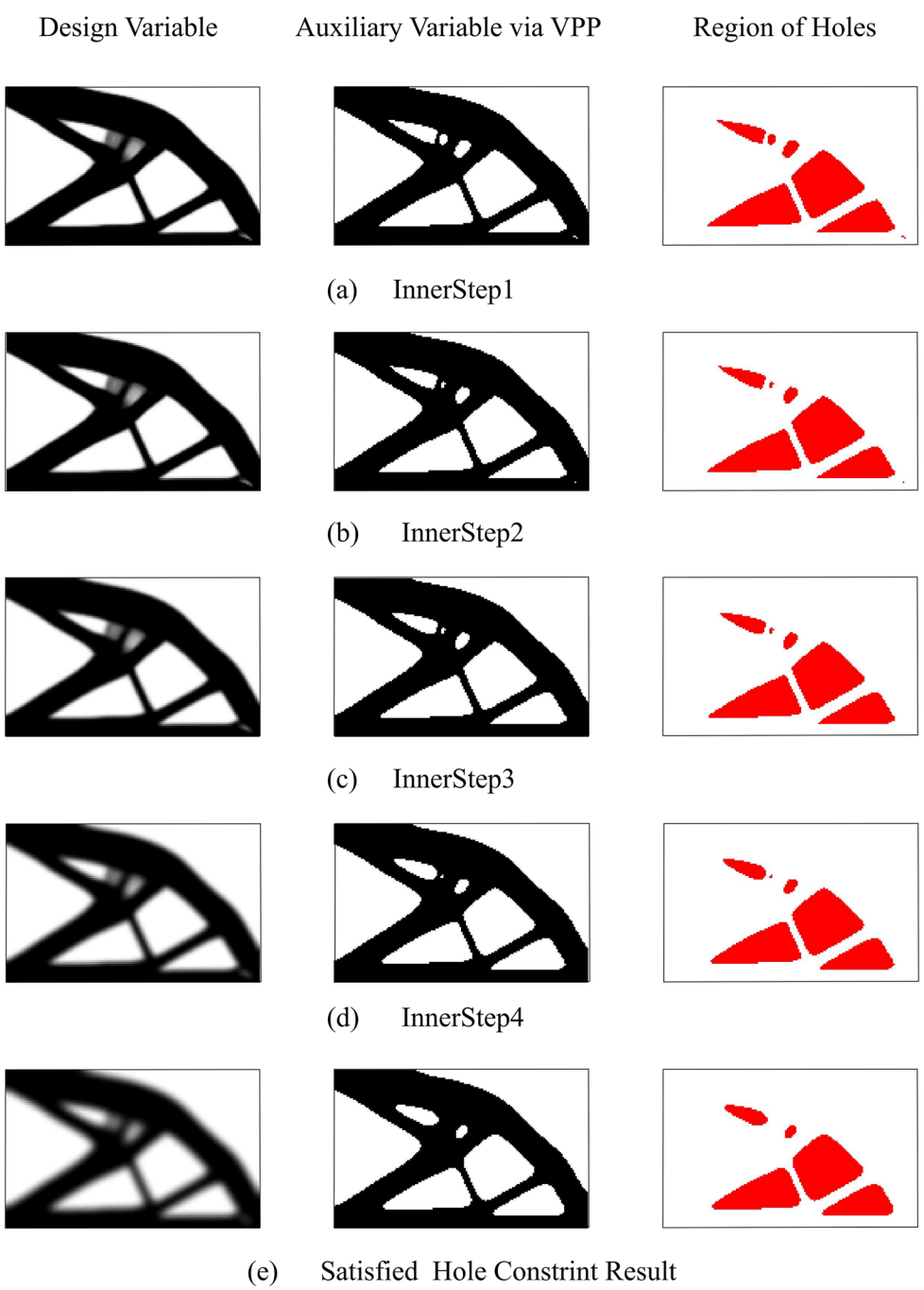

Fig. 13 Variable distribution for the inner loop of the outer iteration for iteration 31; ρ_A is the initial value of inner loop in **(a)**; and $\rho_B \sim \rho_E$ is the design variable for **(b)** $\sim$ **(e)**;$\rho_B = H^{r_1=1.1} * \rho_A$, $\rho_C = H^{r_2=2.1} * \rho_B$; $\rho_D = H^{r_3=3.56} * \rho_C$; $\rho_E = H^{r_4=5.27} * \rho_D$, and ρ_E would be the initial value for next upgrade procedure

Table 1 Strain energy of the optimized results under different hole constraints for the design problem shown in Fig. 1a

Hole 0	Hole 1	Hole 2	Hole 3	Hole 4	Hole 5
50.127	46.121	45.848	45.454	45.175	45.080
Hole 6	Hole 7	Hole 8	Hole 9	Hole 10	Hole 11
45.080	45.093	45.144	45.182	45.228	45.190

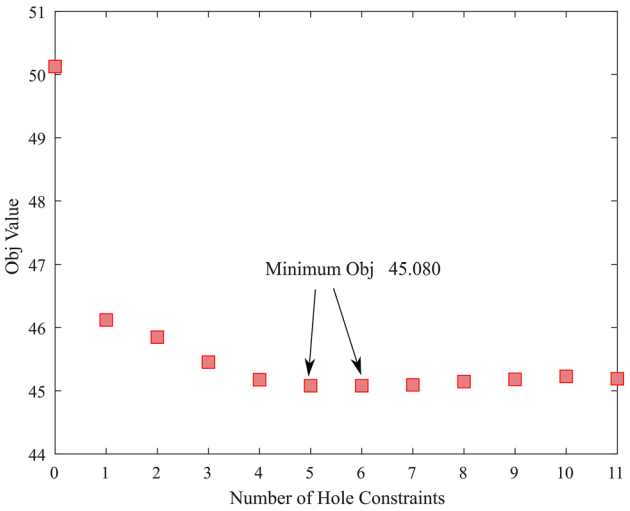

Fig. 14 Calculated strain energy and corresponding hole constraint diagram for Fig. 1a

non-tightly support constrained problem is not discussed. For multiple constraints or multiple loading conditions, it is necessary to further discuss, for example, linking the MMA algorithm to solve the optimization problem.

The discrete 0–1 expression of auxiliary design variable proposed in this paper is simply implemented using the volume preserving projection method. It is known that other more advanced discrete projection methods could also work for this algorithm. For example, one could use volume preserving Heaviside function (Wang et al., 2010; Xu et al., 2009; Li and Khandelwal, 2015; Ferrari and Sigmund, 2020).

The convergence speeds of the algorithm in this paper depends on the *ratio* in the design space progressive restriction method and the target maximum hole constraint number. If one wants to obtain the obvious 0–1 distribution parameter within 250 iteration steps, the proportional minimum should be selected larger than $0.5/250 = 0.002$. If the total maximum iteration number is 200, and the *ratio* equals to 0.01, then after 50 iterations there would exist elements that satisfy the third equation in Eq. 3. Actually, the design space restriction method proposed in this paper is mainly necessary for the cases that hole constraint is chosen as such as 0 or 1, where one has to choose very large filter radius which results in relatively large area with gray elements. Of course, the classical convergent criteria such as the absolute change of the design variable can be also integrated into this proposed numerical model.

With the maximum hole constraints such as the 0-hole constraint, the optimized solution itself is a local optimum with a higher objection value than that of the optimized result without topological constraints. It takes many inner

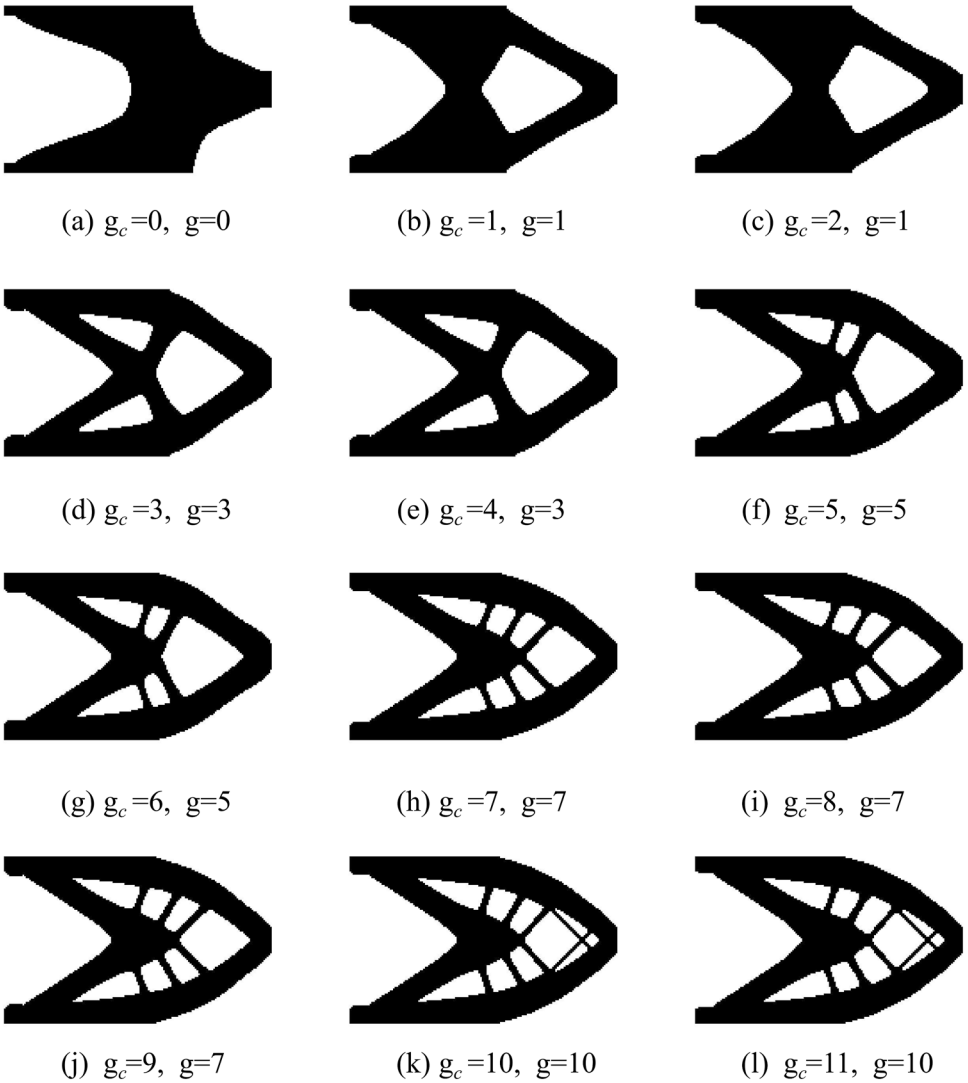

Fig. 15 Hole-constrained results after optimization. The load condition is defined in Fig. 1b, g_c means the maximum hole constraint number, and g is the number of holes of the calculated result

Table 2 Strain energy calculation results under different hole constraints for the case in Fig. 1b

Hole 0	Hole 1	Hole 2	Hole 3	Hole 4	Hole 5
67.981	61.541	61.559	60.444	60.444	60.369
Hole 6	Hole 7	Hole 8	Hole9	Hole10	Hole11
60.376	60.305	60.308	60.325	60.278	60.361

steps to obtain a reasonable local optimum. For the case of Fig. 1a, the strain energy corresponding to the 0-hole constraint is 50.127, while the value for 5-hole optimized solution is 45.080. The strain energy corresponding to 0-hole constraint is 67.981 for the case of Fig. 1b, while the value for the 5-hole optimized solution is 60.369. However, for micro additive manufacturing, a 0-hole constraint solution is easier to manufacture.

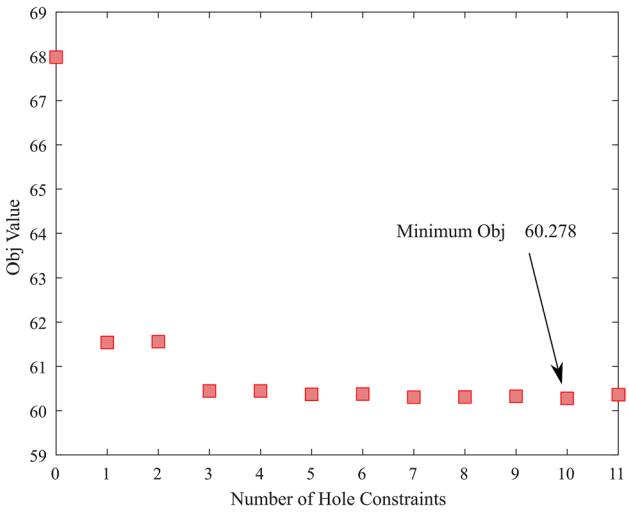

Fig. 16 Calculated strain energy and corresponding hole constraint diagram for Fig. 1b

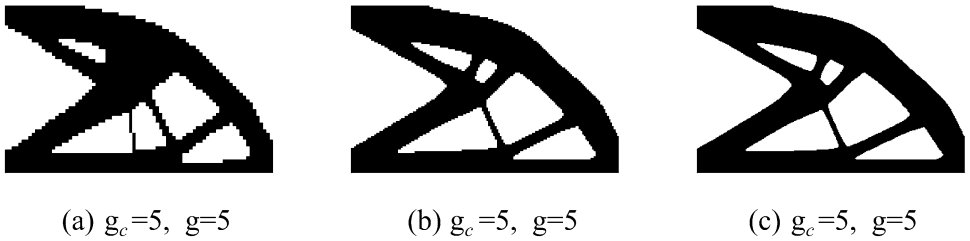

Fig. 17 Five-hole constraint, with different mesh densities (results optimized for Fig. 1a. **a** mesh is 80*50; **b** mesh is 160*100; **c** mesh is 320*200

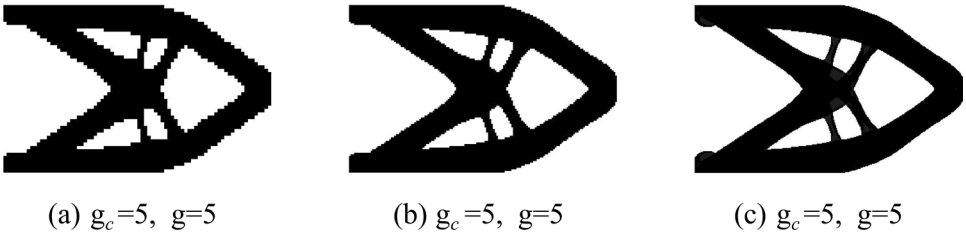

Fig. 18 Five-hole constraint, with different mesh densities (results optimized for Fig. 1b. **a** mesh is 80*50; **b** mesh is 160*100; **c** mesh is 320*200

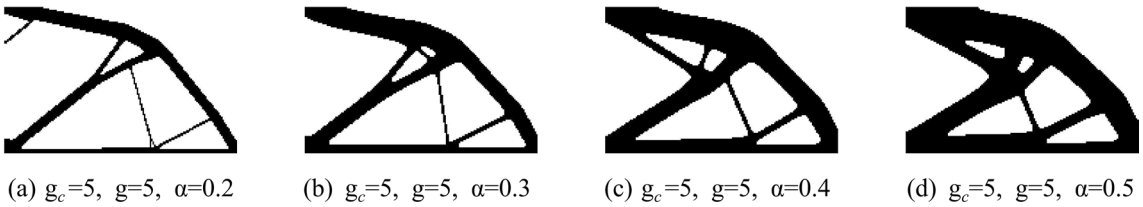

Fig. 19 Five-hole constraint with different volume fractions under a mesh of 160*100; α is the volume fraction

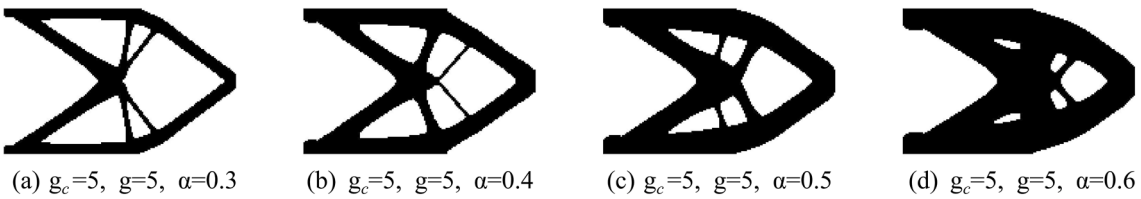

Fig. 20 Five -hole constraint with different volume fractions under a mesh of 160*100; α is the volume fraction

5 Conclusion

Based on the persistence homology, an idea that comes from topological data analysis, this paper shows a topological control strategy methodology with an inequality hole constraint for structural minimum compliance topology optimization in 2D condition. Numerical results of the cantilever beam illustrate that the algorithm can implement genus inequality constraints for various mesh discretization and volume equality constraints. We illustrate that with using the well-known filter method and adding some novel numerical skills, the classical SIMP plus OC strategy can fulfill the specific countable topological constraint.

Acknowledgements This research was funded by the National Natural Science Foundation of China (No. 51675506) and the National Key Research and Development Program of China (No. 2018YFF01011503).

Declarations

Conflict of interest The authors declare that they have no conflicts of interest.

Replication of results We consider that the key algorithm for controlling the number of holes is well explained by the persuasion algorithm chart and can be easily repeated. The strategy of the DSPRM is defined in Sect. Design Space Progressive Restriction Method (DSPRM) and the formulae are listed. For the code of the FBM method, one can refer to topological control work based on the BESO method (Han et al., 2021). The pre-generated filter matrix codes are

modified based on Andreassen's 88-line MATLAB work (Andreassen et al., 2010).

References

Andkjær J, Sigmund O (2011) Topology optimized low-contrast all-dielectric optical cloak. Appl Phys Lett. https://doi.org/10.1063/1.3540687

Andreassen E, Clausen A, Schevenels M, Lazarov BS, Sigmund O (2010) Efficient topology optimization in MATLAB using 88 lines of code. Struct Multidisci Optim 43(1):1–16. https://doi.org/10.1007/s00158-010-0594-7

Bendsøe MP, Sigmund O (2003) 'Topology optimization: theory, methods and applications. Springer

Bendsøe MP, Kikuchi N (1988) Generating optimal topologies in structural design using a homogenization method. Comput Methods Appl Mech Eng 71(2):197–224

Carlsson, G. (2009) Topology and data. *Bull. Amer Math Soc*

Carlsson, G. (2020) Persistent Homology and Applied Homotopy Theory. doi: https: //arxiv.org/abs/2004.00738.

Deng Y, Zhang P, Liu Y, Wu Y, Liu Z (2013) Optimization of unsteady incompressible Navier-stokes flows using variational level set method. Int J Numer Meth Fluids 71(12):1475–1493. https://doi.org/10.1002/fld.3721

Edelsbrunner, H., & Harer, J. (2008). Persistent homology—a survey

Edelsbrunner, H. (2014). A Short Course in Computational Geometry and Topology. Springer International Publishing.

Ferrari F, Sigmund O (2020) A new generation 99 line Matlab code for compliance topology optimization and its extension to 3D. Struct Multidisci Optim 62(4):2211–2228. https://doi.org/10.1007/s00158-020-02629-w

Fugacci, U., Scaramuccia, S., Iuricich, F., & De Floriani, L. (2016). Persistent homology: a step-by-step introduction for newcomers.

Guest JK (2008) Imposing maximum length scale in topology optimization. Struct Multidisci Optim 37(5):463–473. https://doi.org/10.1007/s00158-008-0250-7

Guest JK (2015) Optimizing the layout of discrete objects in structures and materials: a projection-based topology optimization approach. Comput Methods Appl Mech Eng 283:330–351. https://doi.org/10.1016/j.cma.2014.09.006

Guest JK, Prévost JH, Belytschko T (2004) Achieving minimum length scale in topology optimization using nodal design variables and projection functions. Int J Numer Meth Eng 61(2):238–254. https://doi.org/10.1002/nme.1064

Guest JK, Asadpoure A, Ha S-H (2011) Eliminating beta-continuation from Heaviside projection and density filter algorithms. Struct Multidisci Optim 44(4):443–453. https://doi.org/10.1007/s00158-011-0676-1

Guest, J., & Prevost, J. (2006). A Penalty Function for Enforcing Maximum Length Scale Criterion in Topology Optimization. *11th AIAA/ISSMO Multidisciplinary Analysis and Optimization Conference*: American Institute of Aeronautics and Astronautics doi:https://doi.org/10.2514/6.2006-6938

Han H, Guo Y, Chen S, Liu Z (2021) Topological constraints in 2D structural topology optimization. Struct Multidisci Optim 63(12):1–20

Joakim, Petersson, and, Ole, & Sigmund (1998). Slope constrained topology optimization. *International Journal for Numerical Methods in Engineering*

Kawamoto A, Matsumori T, Yamasaki S, Nomura T, Kondoh T, Nishiwaki S (2010) Heaviside projection based topology optimization by a PDE-filtered scalar function. Struct Multidisci Optim 44(1):19–24. https://doi.org/10.1007/s00158-010-0562-2

Kim H, Querin O, Steven GP, et al (2000) A method for varying the number of cavities in an optimized topology using evolutionary structural optimization. Struct Multidisci Optim 19(2):140–147

Lazarov BS, Sigmund O (2011) Filters in topology optimization based on Helmholtz-type differential equations. Int J Numer Meth Eng 86(6):765–781. https://doi.org/10.1002/nme.3072

Lazarov BS, Wang F (2017) Maximum length scale in density based topology optimization. Comput Methods Appl Mech Eng 318:826–844. https://doi.org/10.1016/j.cma.2017.02.018

Lazarov BS, Wang F, Sigmund O (2016) Length scale and manufacturability in density-based topology optimization. Arch Appl Mech 86(1–2):189–218. https://doi.org/10.1007/s00419-015-1106-4

Li L, Khandelwal K (2015) Volume preserving projection filters and continuation methods in topology optimization. Eng Struct 85:144–161. https://doi.org/10.1016/j.engstruct.2014.10.052

Lin Z, Liu V, Pestourie R, Johnson SG (2019) Topology optimization of freeform large-area metasurfaces. Opt Express 27(11):15765–15775. https://doi.org/10.1364/OE.27.015765

Liu S, Quhao LI, Chen W, Tong L, Cheng G (2015) An identification method for enclosed voids restriction in manufacturability design for additive manufacturing structures. Front Mech Eng 10(002):126–137

Otter N, Porter MA, Tillmann U, Grindrod P, Harrington HA (2017) A roadmap for the computation of persistent homology. EPJ Data Sci 6(1):17. https://doi.org/10.1140/epjds/s13688-017-0109-5

Poulsen TA (2003) A new scheme for imposing a minimum length scale in topology optimization. Int J Numer Meth Eng 57(6):741–760. https://doi.org/10.1002/nme.694

Sigmund O (2001) A 99 line topology optimization code written in Matlab. Struct Multidisc Optim 21(2):120–127

Sigmund. (2004). Topology optimization. Springer

Wang F, Lazarov BS, Sigmund O (2010) On projection methods, convergence and robust formulations in topology optimization. Struct Multidisci Optim 43(6):767–784. https://doi.org/10.1007/s00158-010-0602-y

Xu S, Cai Y, Cheng G (2009) Volume preserving nonlinear density filter based on heaviside functions. Struct Multidisci Optim 41(4):495–505. https://doi.org/10.1007/s00158-009-0452-7

Zhao Z-L, Zhou S, Cai K, Min Xie Y (2020) A direct approach to controlling the topology in structural optimization. Comput Struct. https://doi.org/10.1016/j.compstruc.2019.106141

Zhou M, Lazarov BS, Sigmund O (2014) Topology optimization for optical projection lithography with manufacturing uncertainties. Appl Opt 53(12):2720–2729. https://doi.org/10.1364/AO.53.002720

Zhou M, Lazarov BS, Wang F, Sigmund O (2015) Minimum length scale in topology optimization by geometric constraints. Comput Methods Appl Mech Eng 293:266–282. https://doi.org/10.1016/j.cma.2015.05.003